# Ligand-based pharmacophore model of N-Aryl and N-Heteroaryl piperazine α1A-adrenoceptors antagonists using GALAHAD

Xin Zhao [a,b], Mu Yuan [a,*], Biyun Huang [a], Hong Ji [a], Liu Zhu [a]

[a] Pharmaceutical Research Center, Guangzhou Medical College, Guangzhou, Guangdong 510182, China
[b] Department of Food and Bioengineering, Guangdong Industry Technical College, Guangzhou, Guangdong 510300, China

## ARTICLE INFO

## ABSTRACT

Computer aided drug discovery for selective antagonism effects on α1A subtypes of G-protein coupled receptors are important in the treatment of benign prostatic hyperplasia (BPH). Ligand-based pharmacophore models of N-Aryl and N-Heteroaryl piperazine α1A-antagonists were developed using two separate training sets. Pharmacophore models were generated using the flexible align method within the GALAHAD module, implemented in SYBYL8.1 software. The most significant pharmacophore hypothesis, characterized by the conflicting demands of maximizing pharmacophore consensus, maximizing steric consensus, and minimizing energy, consisted of one positive nitrogen center, one donor atom center, two acceptor atom centers, and two hydrophobic groups. The most active compound in each class training set showed a good fit with all features of the pharmacophore proposed. The resulting models also had something in common with the hypothesis using the Catalyst software reported in other publications. These α1A pharmacophore models could predict compounds well, both in the training set and the test set. The pharmacophore models were also validated by an external dataset using a portion of the ZINC database. A 3D-QSAR model using the pharmacophore model to align the compounds was established in this study. The CoMFA model with the cross-validated $q^2$ value of 0.735 revealed that the model was valid. Our research provides a valuable tool for designing new therapeutic compounds with desired biological activity.

© 2010 Elsevier Inc. All rights reserved.

## 1. Introduction

Benign prostatic hyperplasia (BPH) is a common disease in the aging male population (40 years and older) that has attracted worldwide attention [1]. It is characterized by obstructive and irritating symptoms and significantly compromises the quality of life of patients. The BPH symptoms are associated with the prostate smooth muscle cells [2].

A physiopathology study by Caine [3] has provided evidence that prostate smooth muscles are regulated by the sympathetic nerve system through α1-adrenoceptors (α1-ARs). The α1-ARs are members of a superfamily of seven trans-membrane G-protein coupled receptors (GPCR). Recent molecular cloning studies have demonstrated that α1-ARs are not a homogeneous population. When characterized by their functional, radioligand binding, and biochemical properties, they can be separated into three distinct subtypes, designated α1A, α1B and α1D [4]. The α1A-ARs are the predominant receptors causing contraction of the prostate smooth muscle and are thought to result in BPH [5].

A recent paper has reviewed the current research on the discovery and evaluation of a variety of chemically diverse structures as selective antagonists of α1-ARs and α1-ARs subtypes [6]. The different agents can be separated into nine claimed classes with N-Aryl and N-Heteroaryl piperazine derivatives representing particularly important categories. Successful pharmacophore models for α1-ARs antagonists have been reported with a number of different methods and a minimal α1A-subtype pharmacophore, based on four strong bioactivity compounds, has been generated by Bremner et al. [7]. This pharmacophore, generated using Catalyst, consists of three features including a positive charge in the middle of the system, a hydrogen-bond acceptor group, and an aromatic ring system at the opposite end of the molecule. A similar model has been described by Li et al. [8], using the HypoGen module and based on 30 compounds with six orders of magnitude for the antagonistic affinity of α1A-ARs. The features of this model include: one positive ionizable group, one hydrogen-bond donor, one aromatic ring, and one hydrophobic group. Using Catalyst, MacDougall and Griffith also developed a ligand-based pharmacophore hypothesis based on α1A-selective antagonists from the literature [9]; this four-feature pharmacophore was developed for the α1A-subtype-selective antagonists. These pharmacophore models are universally applicable, specifically in the area of virtual screening

* Corresponding author. Tel.: +86 20 81340272; fax: +86 20 81340272.
E-mail address: mryuanmu@yahoo.com.cn (M. Yuan).

of commercial databases and the discovery and optimization of lead compounds. However, these previously reported pharmacophores models have a maximum of only four-feature pharmacophore. The use of these models for candidate drug screening may be limited.

GALAHAD (Genetic Algorithm with Linear Assignment of Hypermolecular Alignment of Datasets) uses Tripos' proprietary technology to generate a pharmacophore hypothesis model. It is also a convenient method for finding a pharmacophore and aligning ligand molecules that bind at a common target site. The GALA-HAD program works in two stages. First, a genetic algorithm (GA) is used to identify a set of ligand conformations that minimizes ligand strain energy while maximizing pharmacophore multiplet similarity between ligands. Pharmacosteric similarity is maximized at the same time, via flexible alignment of the 3D structure. Then, rigid-body alignment overlays the ligands in Cartesian space, and the best models are generated [10].

The aim of this study is to obtain a pharmacophore model based on N-Aryl and N-Heteroaryl piperazine derivatives that could provide a rational hypothetical picture of the chemical features responsible for the $\alpha_{1A}$-AR antagonistic activity of these compounds. Basis of this pharmacophore knowledge, virtual screening of databases and lead compounds optimization can be done using 3D-QSAR methods to develop new and potentially more active candidates for the treatment of BPH.

## 2. Methodology

The compounds were separated into two classes based on the spacing of N-Aryl and N-Heteroaryl piperazine, as noted by Klabunde and Evers [11]. Each training set consisted of eight $\alpha_{1A}$-AR antagonists, obtained from published data (see Table 1). The dataset was refined by removing similar compounds with similar affinities, in order to avoid redundancy of information. The affinity value for $\alpha_{1A}$-AR compounds were reported as $K_i$ values in the training set, and were measured using competition assays of recombinant receptors expressed in cell lines; all $K_i$ values were changed into p$K_i$ values for generating pharmacophore hypotheses. All structures in the training sets were built and their 3D structures were generated using CONCORD. The structures were then energy minimized to the closest local minimum under the Tripos force field, with Gasteiger-Huckel atomic partial charges; using SYBYL 8.1 molecular modeling software on a HP xw9400 workstation equipped with AMD® Opteron 2.8GHz processors.

Pharmacophore models were generated and analyzed using the GALAHAD module in SYBYL8.1 with the flexible alignment method implemented in our protocol. All of the ligands were aligned with each other with a population size value of 50, a maximum generation value of 70 and the value of molecular required hitting was 6. Except as otherwise noted, default parameters were used for the GALAHAD runs with five feature types – ① positive nitrogen, ② negative center, hydrogen bond ③ donor and ④ acceptor atoms, ⑤ hydrophobic center – taken into consideration.

The predictive power of these pharmacophore models for selective $\alpha_{1A}$-AR antagonists was explored. The $\alpha_{1A}$-AR testing set consisted of 8 antagonists from various structural families and with varying degrees of affinity (see Table 1). All molecules in the test set were also built and treated like molecules in the training set. All compounds were aligned with the best template model using GALAHAD and each pharmacophore was regressed against the training sets, then the active values were predicted in the training and test sets based on linear regression. To evaluate the accuracy of the predicted affinities, the error was calculated as the ratio between experimentally-derived affinities and affinities pre-

dicted by SYBYL, with a negative sign if the experimental activity was higher than that predicted.

The pharmacophore models ware validated using a portion of the ZINC database that was seeded with known compounds not used to construct the models performed with the SYBYL software. Nevertheless, the size of the database should be restricted as much as possible and first selection of drugable compounds within the ZINC database was thus conducted. The aryl-piperazine moiety was added to the parameters used for the query [24]. A small database containing 260 compounds were loaded in the SYBYL environment, which contains 14 $\alpha_{1A}$-AR antagonists. The conformers of each compound were then filtered by the pharmacophore model using UNITY 3D search module. To be considered as a hit the compound has to fit all the features of the pharmacophore.

A 3D-QSAR model using the pharmacophore model to align the compounds of interest was established in this study. The structures and affinity value of N-Aryl and N-Heteroaryl piperazine compounds were also collected from the literatures [12,13,17,18,25]. This collection included 24 compounds distributed in 4 series (Fig. 1), in which 20 compounds constituted the training set and the remaining 4 compounds were chosen as the test (see Table 2). All compounds were also built and then energy minimized under the Tripos' force field with Gasteiger-Huckel atomic partial charges; and then aligned with the best template model using 'Align molecules to Template Individually' mode with GALAHAD.

A comparative molecular field analysis (CoMFA) has been performed to evaluate the steric and electrostatic fields implemented in SYBYL. The CoMFA steric and electrostatic fields were calculated at grid points using the Lennard–Jones and Coulomb potential functions of the Tripos' field. A $sp3$ carbon atom with a charge of +1.0, a Van der Waals radius of 1.52 Å was probed on 2 Å spaced lattice, which extended 4 Å units beyond the dimensions of aligned molecules in all directions. The PLS method was used to explore a linear correlate between the CoMFA fields and biological activity values [26,27]. The cross-validated analysis was performed using the leave-one-out method. The leave-many-out procedure was performed to ensure the reproducibility of $q^2$. The cross-validated $q^2$ that resulted in minimal number of components and lowest standard error of prediction was accepted. After that, non-cross-validation was performed to derive the final PLS regression models.

## 3. Results and discussion

Klabunde and Evers divided high-affinity $\alpha_{1A}$-AR antagonists into two classes [11]. Class I antagonists were characterized by a $\pi$-nitrogen positioned 2–3 bond lengths from an aromatic ring and 6–7 bond lengths from a second aromatic ring. In contrast, Class II antagonists exhibited two aromatic rings; both positioned 2–4 bond lengths from $\pi$-nitrogen. However, many of compounds that have $\alpha_{1A}$-AR antagonist activity do not follow the initial classification. These 'outliers' compounds may not have two aromatic rings, or the number of bond lengths between aromatic rings and the positively ionizable nitrogen falls outside the parameters for classification. Base on Klabunde and Evers's definition, we separated compounds into two classes without using the same bond length limits of the $\pi$-nitrogen position with respect to the two aromatic rings.

Twenty pharmacophore models were generated by GALAHAD for each class, because of a multi-objective fitness function used in the genetic algorithm; each of these represented a different trade-off among the competing criteria [28]. Table 3 lists the parameters of each model, and Fig. 2 shows the alignments of $\alpha_{1A}$-ARs ligands obtained using GALAHAD. The models seldom achieved optimum values simultaneously in all parameters. The most significant pharmacophore hypothesis was characterized by

**Table 1**
Structures of $\alpha_{1A}$-ARs in the training and test set and their experimental and predicted biological affinities for cloned human $\alpha_{1A}$-ARs.

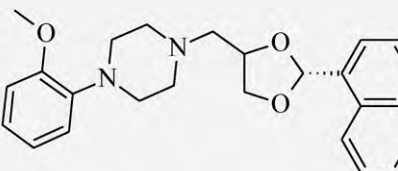| Compound name[a] | Molecular structure | Experimental $K_i$ (nM) | Experimental $pK_i$[b] | Predicted $K_i$ (nM) | Error[c] |
|---|---|---|---|---|---|
| Training set | | | | | |
| **A1** [12] | | 0.16 | 9.80 | 0.26 | +1.63 |
| **A2** [13] | | 0.52 | 9.28 | 0.66 | +1.27 |
| **A3** [14] | | 0.61[d] | 9.21 | 0.53 | −1.15 |
| **A4** [7] | | 1.00 | 9.00 | 0.85 | −1.18 |
| **A5** [12] | | 1.02 | 8.99 | 0.77 | −1.32 |
| **A6** [7] | | 2.00 | 8.70 | 1.98 | −1.01 |
| **A7** [13] | | 2.38 | 8.62 | 1.82 | −1.31 |
| **A8** [15] | | 9.30 | 8.03 | 10.93 | +1.18 |

Table 1 (*Continued* ).
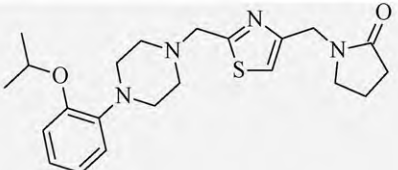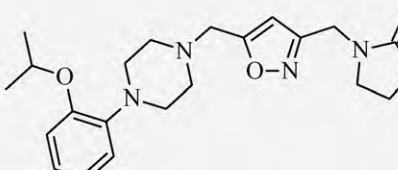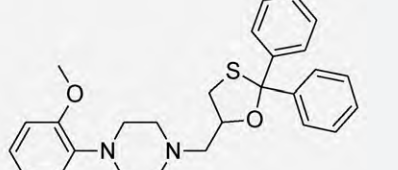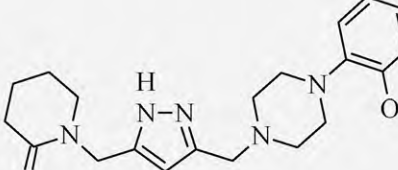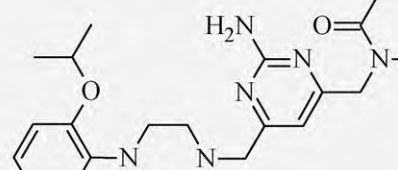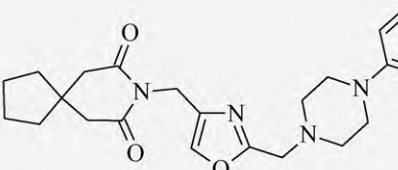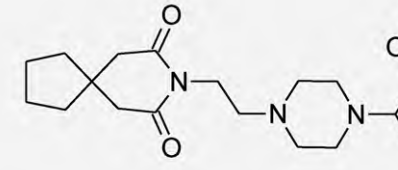
| Compound name[a] | Molecular structure | Experimental $K_i$ (nM) | Experimental $pK_i$[b] | Predicted $K_i$ (nM) | Error[c] |
|---|---|---|---|---|---|
| **B1** [16] | | 0.9 | 8.92 | 0.78 | −1.15 |
| **B2** [16] | | 1.1 | 8.96 | 1.36 | +1.24 |
| **B3** [17] | | 2.0[d] | 8.69 | 4.16 | +2.08 |
| **B4** [18] | | 2.1 | 8.68 | 1.33 | −1.58 |
| **B5** [17] | | 8.0[d] | 8.10 | 14.83 | +1.85 |
| **B6** [18] | | 79 | 7.10 | 67 | −1.79 |
| **B7** [16] | | 82 | 7.09 | 50 | −1.64 |
| **B8** [7] | | 250[d] | 6.42 | 257 | +1.03 |

Table 1 (Continued).
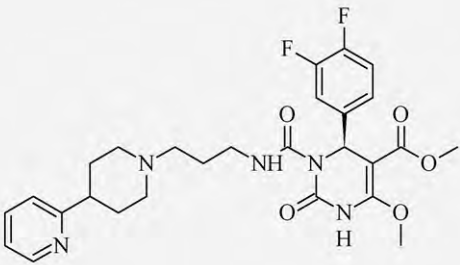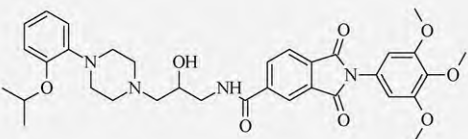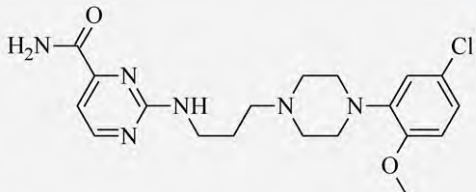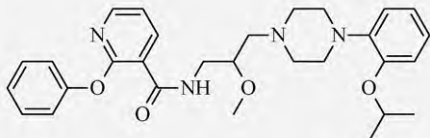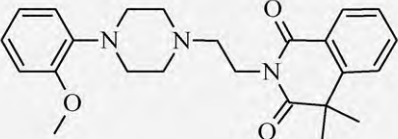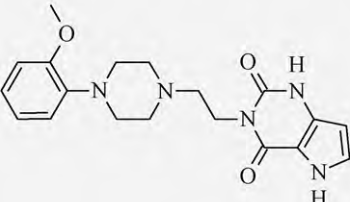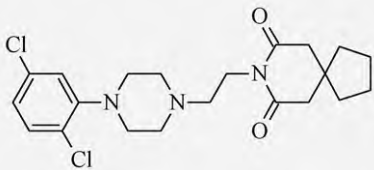
| Compound name[a] | Molecular structure | Experimental $K_i$ (nM) | Experimental $pK_i$[b] | Predicted $K_i$ (nM) | Error[c] |
|---|---|---|---|---|---|
| Test set | | | | | |
| A9 [19] |  | 0.36 | 9.44 | 0.41 | +1.14 |
| A10 [12] |  | 1.22 | 8.91 | 1.82 | +1.49 |
| A11 [7] |  | 2.00 | 8.70 | 2.09 | +1.05 |
| A12 [13] |  | 2.37 | 8.63 | 1.81 | −1.31 |
| B9 [20] |  | 0.5 | 9.30 | 0.33 | −1.52 |
| B10 [21] |  | 1 | 9.00 | 0.76 | −1.32 |
| B11 [22] |  | 2.31 | 8.64 | 2.42 | +1.05 |

Table 1 (*Continued*).

| Compound name[a] | Molecular structure | Experimental $K_i$ (nM) | Experimental $pK_i$[b] | Predicted $K_i$ (nM) | Error[c] |
|---|---|---|---|---|---|
| **B12** [23] |  | 128 | 6.89 | 151 | +1.18 |

[a] A: Class I antagonists; B: Class II antagonists.
[b] Expressed as $pK_i$, where $K_i$ was the affinity of compounds toward $\alpha_{1A}$-ARs in nM and the equation was $pK_i = \log(1/K_i)$;.
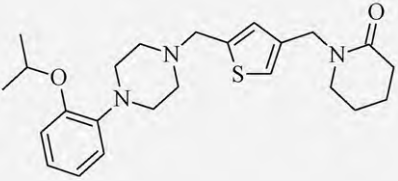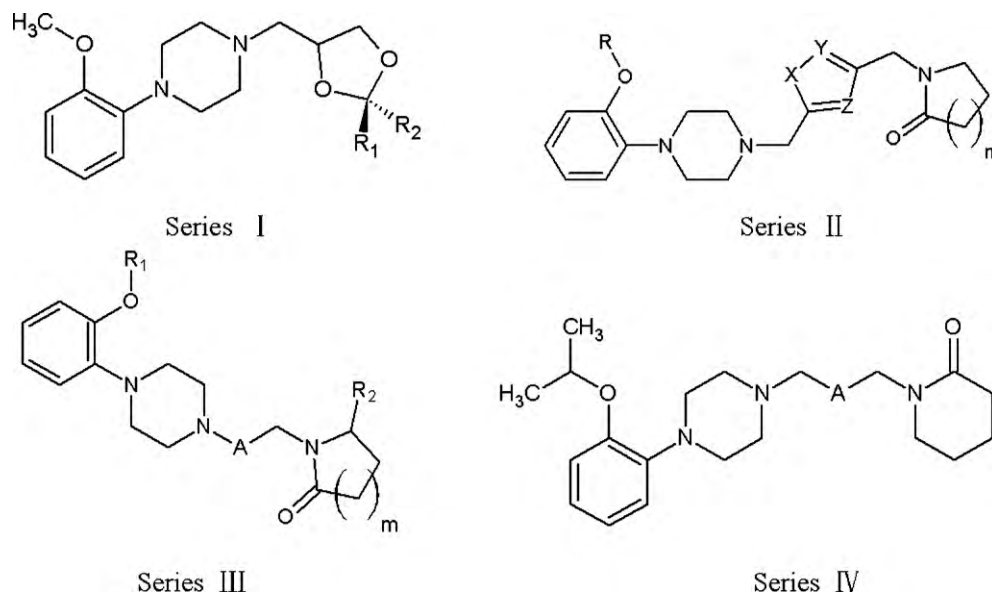[c] Error was calculated as the ratio between experimental affinities and predicted affinities, with a negative sign if the experimental activity was higher than that predicted.
[d] $pK_i$ value was shown in the publication, and $K_i$ values was changed from $pK_i$ value.



Series I    Series II

Series III    Series IV

**Fig. 1.** Four series structural types of the collected compounds.

**Table 2**
Experimental and predicted $pK_i$ and residuals obtained by the CoMFA model for 20 compounds in the training set and 4 compounds in the test set[a].

| Series | Cpd. | Structure | Exp. $pK_i$ | Pred. $pK_i$ | Residual |
|---|---|---|---|---|---|
| I | **1** | $R_1$ = naphthyl-1-yl, $R_2$ = H | 7.44 | 7.97 | −0.53 |
| | **2** | $R_1$ = H, $R_2$ = naphthyl-1-yl | 8.1 | 8.14 | −0.04 |
| | **3**[b] | $R_1$ = Ph, $R_2$ = H | 7.54 | 7.97 | −0.43 |
| | **4** | $R_1$ = H, $R_2$ = Ph | 8.57 | 8.33 | 0.24 |
| | **5** | $R_1$ = naphthyl-2-yl, $R_2$ = H | 7.82 | 7.81 | 0.01 |
| II | **6** | R = $i$-Pr, X = S, Y = H, Z = H, $m$ = 2 | 9.3 | 8.77 | 0.53 |
| | **7** | R = $i$-Pr, X = S, Y = H, Z = H, $m$ = 3 | 8.74 | 8.68 | 0.06 |
| | **8** | R = $i$-Pr, X = S, Y = H, Z = N, $m$ = 1 | 9.05 | 8.71 | 0.34 |
| | **9**[b] | R = $i$-Pr, X = S, Y = H, Z = N, $m$ = 2 | 8.92 | 8.73 | 0.19 |
| | **10** | R = $i$-Pr, X = O, Y = N, Z = H, $m$ = 1 | 8.96 | 8.58 | 0.38 |
| | **11** | R = Me, X = H, Y = H, Z = S, $m$ = 1 | 7.4 | 7.36 | 0.04 |
| | **12** | R = Me, X = H, Y = H, Z = S, $m$ = 2 | 7.85 | 7.40 | 0.45 |
| | **13** | R = Me, X = H, Y = H, Z = S, $m$ = 3 | 7.74 | 7.40 | 0.34 |
| | **14** | R = Ph, X = O, Y = N, Z = H, $m$ = 3 | 7.07 | 6.96 | 0.11 |
| III | **15**[b] | $R_1$ = Me, A = $(CH_2)_3$NHCO, $R_2$ = H, $m$ = 2 | 7.01 | 7.48 | −0.47 |
| | **16** | $R_1$ = $i$-Pr, A = $(CH_2)_3$NHCO, $R_2$ = H, $m$ = 2 | 9.18 | 8.77 | 0.41 |
| | **17** | $R_1$ = $i$-Pr, A = $C_2H_4$NHCO, $R_2$ = $CO_2$Et, $m$ = 2 | 7.7 | 7.39 | 0.31 |
| | **18** | $R_1$ = $i$-Pr, A = $C_2H_4$NHCO, $R_2$ = H, $m$ = 3 | 7.74 | 7.44 | 0.3 |
| | **19** | $R_1$ = $i$-Pr, A = $(CH_2)_2$OCO, $R_2$ = H, $m$ = 2 | 7.42 | 7.66 | −0.24 |
| IV | **20** | A = 3-4,5-dihydroisoxazole-5-yl | 7.05 | 7.32 | −0.27 |
| | **21** | A = 3-isoxazole-5-yl | 7.42 | 7.16 | 0.26 |
| | **22**[b] | A = 5-1-methyl-1H-pyrazole-3-yl | 8.05 | 8.26 | −0.21 |
| | **23** | A = 3-1-methyl-3H-pyrazole-5-yl | 8.43 | 8.48 | −0.05 |
| | **24** | A = 2-amine-6-pyrimidin-4-yl | 8.68 | 8.51 | 0.17 |

[a] The experimental binding affinities toward the $\alpha_1$-AR are expressed as $pK_i$ values. Residuals is the error of cross-validated (training set) or predicted (test set) binding affinities and is defined as ($pK_i$, experimental−$pK_i$, cross-validated/predicted).
[b] The test compound.

**Table 3**
Parameters of $\alpha_{1A}$-ARs pharmacophore models of each class.

| | Class I antagonists | | | | Class II antagonists | | | |
|---|---|---|---|---|---|---|---|---|
| | SPECIFICITY | N_HITS | FEATS | PARETO | SPECIFICITY | N_HITS | FEATS | PARETO |
| MODEL_001 | 3.317 | 6 | 5 | 0 | 3.050 | 7 | 5 | 0 |
| MODEL_002 | 3.779 | 7 | 6 | 0 | 2.167 | 8 | 4 | 0 |
| MODEL_003 | 4.212 | 8 | 6 | 0 | 3.973 | 4 | 6 | 0 |
| MODEL_004 | 3.305 | 5 | 5 | 0 | 3.27 | 7 | 5 | 0 |
| MODEL_005 | 2.843 | 8 | 5 | 0 | 4.233 | 6 | 6 | 0 |
| MODEL_006 | 4.248 | 6 | 6 | 0 | 3.474 | 5 | 4 | 0 |
| MODEL_007 | 3.222 | 8 | 5 | 0 | 3.133 | 7 | 5 | 0 |
| MODEL_008 | 1.301 | 8 | 2 | 0 | 2.147 | 8 | 4 | 0 |
| MODEL_009 | 3.134 | 7 | 5 | 0 | 2.989 | 6 | 4 | 0 |
| MODEL_010 | 2.037 | 7 | 3 | 0 | 3.949 | 5 | 6 | 0 |
| MODEL_011 | 3.302 | 8 | 5 | 0 | 3.473 | 3 | 4 | 0 |
| MODEL_012 | 3.314 | 7 | 5 | 0 | 2.021 | 4 | 3 | 0 |
| MODEL_013 | 3.126 | 7 | 5 | 0 | 2.086 | 6 | 3 | 0 |
| MODEL_014 | 2.106 | 6 | 3 | 0 | 4.031 | 7 | 6 | 0 |
| MODEL_015 | 1.301 | 7 | 2 | 0 | 3.042 | 4 | 5 | 0 |
| MODEL_016 | 2.209 | 8 | 4 | 0 | 2.02 | 8 | 3 | 0 |
| MODEL_017 | 3.659 | 5 | 4 | 0 | 3.318 | 4 | 4 | 0 |
| MODEL_018 | 2.108 | 6 | 3 | 0 | 2.764 | 5 | 3 | 0 |
| MODEL_019 | 1.301 | 8 | 2 | 0 | 1.301 | 8 | 2 | 0 |
| MODEL_020 | 2.832 | 7 | 5 | 1 | 2.526 | 6 | 3 | 0 |

the conflicting demands of maximizing pharmacophore consensus, maximizing steric consensus, and minimizing conformer potential energy.

### 3.1. Results for Class I

SPECIFICITY was a logarithmic indicator of the expected discrimination for each model, based on the number of features it contained, their distribution across any partial match constraints, and the degree to which the features were separated in space. Good models usually have a high value of SPECIFICITY. For Class I antagonists, MODEL_006, MODEL_003 and MODEL_002 had high SPECIFICITY values of 4.248, 4.212 and 3.779, respectively. These models gave reasonable pharmacophore models. The N_HITS column shows the number of ligands the pharmacophore 'hit' in the training set, and many of the models matched at least 6 ligands

in the dataset. The value in the FEATS column indicates the total number of features possessed by each model. Out of 20 models, 14 models had four or more features. The values in the PARETO column indicate whether a model was superior to other models based on the four criteria of energy, sterics, H-bond, and MOL_QRY. All of the Class I models retained had a PARETO rank value of 0, except for MODEL_020.

Three models had the same number of pharmacophore features; however, MODEL_006 had a different pharmacophore feature. MODEL_006 had one more hydrophobic center, and one less acceptor atom center with a higher energy score than the others (see Table 4). Usually, model selection was based on steric and energy criteria as a basis. The best model with high SPECIFICITY value often had the higher steric score and lower energy value [29]. MODEL_002 had a slightly lower energy value (20.3 kcal/mol) and a slightly higher steric score (4763.1) than



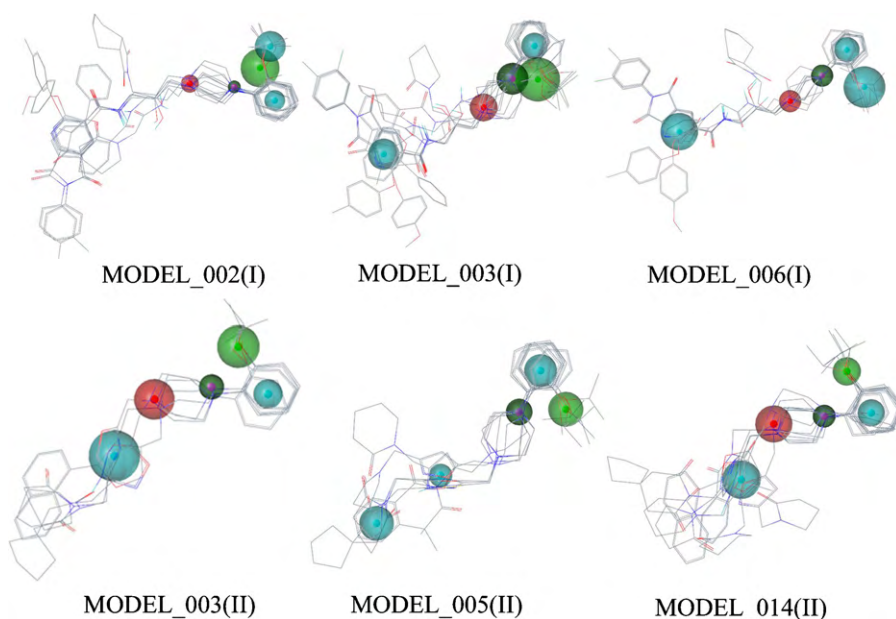**Fig. 2.** Alignments of $\alpha_{1A}$-ARs ligands obtained using GALAHAD. Hypothesis models were initially generated with donor atom (magenta); acceptor atom (green); hydrophobic center (cyan); positive nitrogen (red) as possible features. (I) shows the top 3 specificity models of the class I antagonists in the training set. (II) shows the top 3 specificity models of the class II antagonists in the training set.

**Table 4**
Parameters of pharmacophore features for the top 3 specificity models of each class.

| | Energy[a] | Sterics | H-bond | Pharmacophore features[b] |
|---|---|---|---|---|
| **Class I antagonists** | | | | |
| MODEL_002 | 20.3 | 4763.1 | 505.5 | D:1 A:2 H:2 P:1 |
| MODEL_003 | 92.9 | 4903.5 | 507.3 | D:1 A:2 H:2 P:1 |
| MODEL_006 | 4958.7 | 5638 | 512 | D:1 A:1 H:3 P:1 |
| **Class II antagonists** | | | | |
| MODEL_003 | 1605.1 | 1163.9 | 247.5 | D:1 A:2 H:2 P:1 |
| MODEL_005 | 14,928,578 | 1243.2 | 254.4 | D:1 A:2 H:3 |
| MODEL_014 | 15.42 | 947.8 | 219.3 | D:1 A:2 H:2 P:1 |

[a] The units is kcal/mol.
[b] A, acceptor atom; D, donor atom; H, hydrophobic center; P, positive nitrogen.

MODEL_003. MODEL_002 also contained the HY–HY–$\pi$ system feature satisfied by the methoxy substituent, the phenyl ring and nitrogen, as well as containing the same characteristics as reported in the literature [30]. However, the whole pharmacophore model only corresponded to the aryl-piperazine part of the compound. The follow-up evaluation will be limited to the use of MODEL_002.

### 3.2. Results for Class II

For Class II antagonists, all of the models had PARETO rank values of 0. Many of the models also matched at least 6 ligands in the dataset and had four or more pharmacophore features. MODEL_005, MODEL_014 and MODEL_003 of Class II had high SPECIFICITY values of 4.233, 4.031, and 3.973, respectively, which provided a worthy pharmacophore models to consider.

Models of Class II with a high SPECIFICITY value had the features of a donor atom, an acceptor atom, a hydrophobic center and a positive ionizable center, with the except for MODEL_005 (see Table 4). In the cases of the $\alpha_{1A}$-AR pharmacophore, the positively charged nitrogen atom has been suggested to play a major role in binding [31–33]. The positive region of the ligand can interact with the acid group of a conserved aspartate acid residue in the binding pockets of $\alpha_{1A}$-ARs. MODEL_005 had the highest energy value of 14,928,578 kcal/mol and was discarded. Much attention should

not be given to any models with very high energies as they may have steric clashes. Compared with MODEL_003, MODEL_014 had a lower energy value and a slightly lower steric score. MODEL_014 also had a high SPECIFICITY value and the same pharmacophore feature orientation as MODEL_003 of the Class I, and could be chosen as the best model.

### 3.3. Comparison of Class I and II results

The pharmacophore features of two classes of compounds are shown in Fig. 3. The distances and angles between pharmacophore features of the two class antagonists are listed in Table 5. The location and the distance of each pharmacophore feature center were consistent with the two types of N-Aryl and N-Heteroaryl piperazine antagonist series. Pharmacophore models generated by GALAHAD contained one donor atom, one positive nitrogen atom, two acceptor atoms, and two hydrophobic centers. In the presented figures, different colored spheres represent the different pharmacophore features: magenta sphere represents hydrogen-bond donor atom (D); green one represents acceptor atom (A); cyan one represents hydrophobic center (H) and red one represents positive nitrogen (P). When one of the green spheres overlapped with a magenta one, this indicated the two features coincided, which was confirmed by the distance value of donor atom (D) to acceptor atom ($A_2$). The trigonal planar nitrogen atom on the piperazine ring can donate hydrogen as well as accept hydrogen bonds.

The resulting models also had something in common with the proposed pharmacophore models using the Catalyst software reported in previous publications. Our pharmacophore models showed the distance from the positive nitrogen to the 'right' hydrophobic center (P-$H_2$) to be 5.46 and 5.48 Å, while Li et al. [8] reported a similar value of 5.296–5.477 Å; while Bremner et al. [7] reported a value of 5.5 Å. The difference in location of the 'left' hydrophobic center in Fig. 3 will lead to the corresponding changes in the angle and distance. The distances between the feature centers (P-$H_1$) of our model were 3.58 and 8.96 Å, which were different from those reported by Li et al. [8] (P-H 5.64 Å). Increasing the spacer connecting the aryl-piperazine moiety to the hydropho-
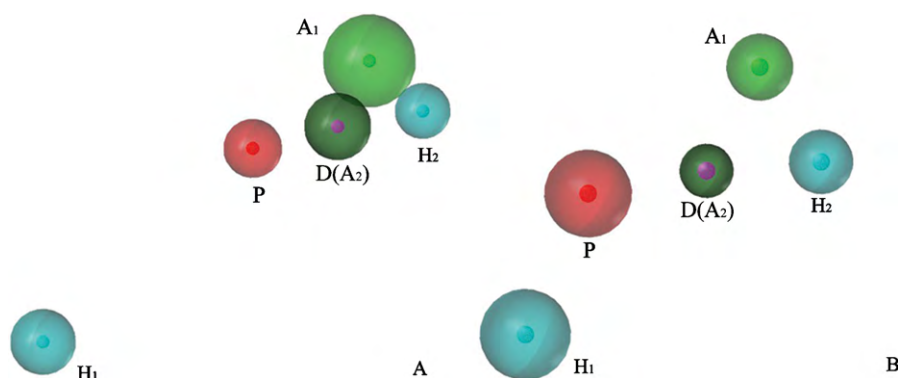


**Fig. 3.** Comparison of two classes of pharmacophore models. The colored spheres correspond to the pharmacophoric features in three-dimensional representations with the following colors: magenta, hydrogen-bond donor atom; green, acceptor atom; cyan: hydrophobic center; red, positive nitrogen. (A) Class I antagonists; (B) Class II antagonists.

**Table 5**
Distances and angles of pharmacophores of two class antagonists.

| Pharmacophore | Distance ranges (Å) and angles (°) between features[a] |
|---|---|
| Class I antagonists | $H_1$–P–D:151.7 $H_1$–P–$A_1$:173.1 $H_1$–$H_2$–$A_1$:75.3 |
| | P–D 2.76 P–$H_1$ 8.96 P–$H_2$ 5.46 P–$A_1$ 4.60 D–$H_1$ 11.47 D–$H_2$ 2.73 D–$A_1$ 2.30 $H_1$–$H_2$ 13.95 $H_1$–$A_1$ 13.54 $A_1$–$H_2$ 2.36 D–$A_2$ 0 |
| Class II antagonists | $H_1$–P–D 145.1 $H_1$–P–$A_1$ 164.8 $H_1$–$H_2$–$A_1$ 80.6 |
| | P–D 2.82 P–$H_1$ 3.58 P–$H_2$ 5.48 P–$A_1$ 4.93 D–$H_1$ 5.68 D–$H_2$ 2.67 D–$A_1$ 2.74 $H_1$–$H_2$ 7.97 $H_1$–$A_1$ 8.23 $A_1$–$H_2$ 2.70 D–$A_2$ 0 |

[a] A: acceptor atom; D: donor atom; H: hydrophobic center; P: positive nitrogen.

(A)                                                                          (B)
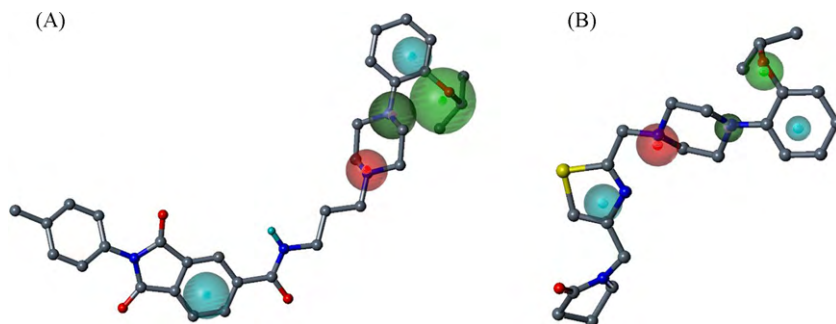


**Fig. 4.** Pharmacophore mappings of the highest affinity compound for each class. The colored spheres correspond to the pharmacophoric features in three-dimensional representations with the following colors: magenta, hydrogen-bond donor atom; green, acceptor atom; cyan: hydrophobic center; red, positive nitrogen. (A) 3D representation of Class I antagonists mapped onto A1; (B) 3D representation of Class II antagonists mapped onto B1.

bic center produced a slight variation in $\alpha_{1A}$-AR affinity [30]. There may be a certain interval range for the length between these groups. Our models had six pharmacophore features and may become more selected in the screening of new candidate compounds, as well as related QSAR calculation.

Compounds A1 and B1, the most active in the training set of each class, showed a good fit with all features of the proposed pharmacophore model shown in Fig. 4. In this case, the positive ionizable sphere was mapped by a $sp^3$ hybridized nitrogen atom, which had the ability to be protonated and thus became positively charged. The donor atom was mapped by the nitrogen atom connected with the benzene ring, which also fit as an acceptor atom center. This could be confirmed by the distance of the donor atom center to the acceptor atom center. Another acceptor atom feature was accommodated by the oxygen atom of the benzene methoxy substituent. There were two hydrophobic features; one was fit by a phenyl plane and the other was fit by the thiazole ring of the heterocyclic portion of the compound A1 or phthalimide portion of the compound B1.

### 3.4. Discussion of results

If the model can forecast the activity of a similar compound structure, that would be one way to check the quantitative correctness of the pharmacophore model. Table 1 shows the experimented and estimated activity for the $\alpha_{1A}$-adrenoceptor in the training and test sets based on the each class's best pharmacophore model. Each pharmacophore model was regressed against the training sets. The correlation values for each regression were 0.902 for Class I and 0.927 for Class II. Each pharmacophore model showed a high correlation to its own dataset. The activities were reported as Ki values spanning from 0.16 to 238 nM.

It appeared from the predictive power that our pharmacophore model was best able to predict the affinities of $\alpha_{1A}$-antagonists that fall into either Class I or II. Out of the 16 compounds in the training set, five compounds in Class I and one compound in Class II were predicted very close to the experimental active (the absolute error value is less than 1.2), while 8 compounds in the test set, one compound in Class I and three compounds in Class II were predicted to be closely active. Raw data of the A10 and A12 did not give configuration information. 'Automated Feature Alignment Module' in GALAHAD was used to deal with these chiral molecules. The final alignment configurations were all R-enantiomer. The errors of the two compounds are higher, which may mean there were a significant relationship between configuration and affinity of these compounds. For Class I antagonists only, the average error was 1.25, while for Class II antagonists only, the average error was 1.33.

Virtual screening was a cost-effective tool in rational drug design for the identification of novel lead compounds. It also could be used to verify the accuracy of the pharmacophore model. For a set of 260 dataset of compounds that contain 14 specific $\alpha_{1A}$-AR antagonists and 246 nonspecific antagonists, there were 25 compounds that matched the pharmacophore using UNITY 3D research. Of these 14 specific $\alpha_{1A}$-AR antagonists, the pharmacophore generated picked 12 compounds. Within 246 nonspecific inhibitors dataset, the model picked 13 molecules, where six compounds had no similarity ensemble approach (SEA) prediction in ZINC database, and the others had other target activity. Hence the enrichment factor calculated over this model generated to the 260 dataset is around 8.9 [34]. These numbers speak of evaluation of the model and ability to pick the specific $\alpha_{1A}$-AR antagonists in the dataset.

A 3D-QSAR using the pharmacophore model to align the compounds was established. The values of p$K_i$ calculated by CoMFA and the residual between experimental and predicted of all the com-

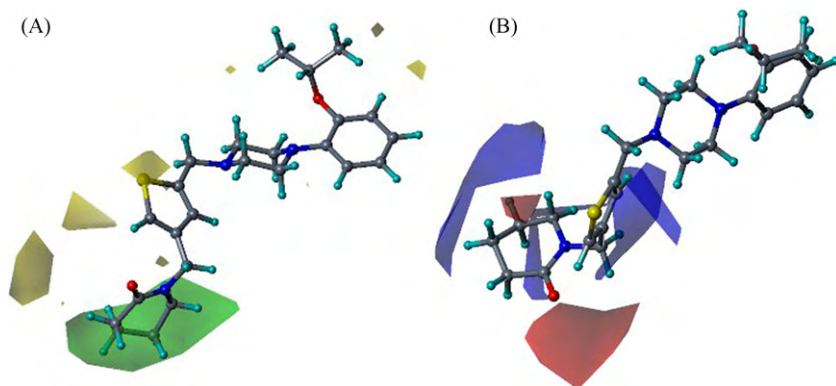(A)                                                                          (B)



**Fig. 5.** CoMFA contour maps with compound 6 as the reference structure. (A) steric contours: scattered green areas are regions where bulky substituents are desirable, while yellow areas are undesirable; (B) electrostatic contours: the red areas are the regions where negative potential is favorable for the activity, while blue areas are unfavorable.

pounds are listed in Table 2, with the graphs in Fig. 5. The CoMFA model yielded satisfactory statistical data with the cross-validated $q^2$ value of 0.735 with six components, which revealed that the model was valid. The non-cross-validated PLS analysis results in a conventional $r^2$ of 0.998, $F = 2514.794$, and a standard error of estimated (SD) of 0.032. These results and the correlation between experimental and predicted activity is good, which also indicates the robustness of the models.

Favored and disfavored cutoff energies were set at the 85th and 15th percentiles for the steric contributions and the electrostatic contributions, the contour maps of the fields included in the CoMFA model were shown in Fig. 5 with compound 6 as a reference structure. The predominant field color for the steric interactions in panel (A) was obviously green. The region beneath the piperidin-2-one side chain was considered as sterically (colored green) favored area. The other three yellow isopleths areas, far from the left side of the piperidin-2-one, flank the sides of the thiophene, reflected a strict decrease in affinity of $\alpha_{1A}$-AR activity. In panel (B), the blue-colored regions showed areas where electropositive charged groups enhance $\alpha_{1A}$-AR affinity. Three blue areas in the vicinity of the protonated piperazine nitrogen, thiophene and piperidin-2-one, indicated different orientation or omission of this functional moiety exerted a negative impact on the binding properties. The electrostatic contour map showed a region of red in particular position of the piperidin-2-one, indicated that electron-rich substituent was beneficial for the binding affinity.

## 4. Conclusion

In the current work, pharmacophore models were successfully generated using two types of phenylpiperazine derivative training sets contain 8 compounds each. Pharmacophores were generated using the GALAHAD Module of SYBYL 8.1 molecular modeling software, and contained one donor atom, one positive nitrogen, two acceptor atoms and two hydrophobic centers. External testing sets of 4 compounds each were successfully predicted by applying the constructed models. Virtual screening of a small databases using of the pharmacophore model was done and a 3D-QSAR using the pharmacophore model to align the compounds was established, which indicated the model was validated.

Using the model information we were able to discover more novel potential molecules that would act as $\alpha_{1A}$-AR antagonists by driving pharmacophore multiple searches of a 3D database. We could also do further QSAR studies on these types of compounds, to find better compounds for benign prostatic hyperplasia treatment.

## Acknowledgements

## Appendix A. Supplementary data

Supplementary data associated with this article can be found, in the online version, at doi:10.1016/j.jmgm.2010.05.002.

## References

[1] A. Tiwari, N.S. Krishna, K. Nanda, A. Chugh, Benign prostatic hyperplasia: an insight into current investigational medical therapies, Exp. Opin. Invest. Drugs 14 (2005) 1359–1372.
[2] K. Natasha, P.L. Juan, B. Andrew, A. Richard, C.J. Stephen, Induction of prostate apoptosis by doxazosin in benign prostatic hyperplasia, J. Urol. 159 (1998) 1810–1815.
[3] M. Caine, Alpha-adrenergic blockers for the treatment of benign prostatic hyperplasia, Atlas. Urol. Clin. 17 (1990) 641–649.
[4] H. Zhong, K.P. Minneman, $\alpha_1$-Adrenoceptor subtypes, Eur. J. Pharmacol. 375 (1999) 261–276.
[5] S. Kaplan, $\alpha$-Blocker therapy: current update, Rev. Urol. 7 (2005) S34–S42.
[6] K.S. Jain, J.B. Bariwal, M.K. Kathiravan, M.S. Phoujdar, R.S. Sahne, B.S. Chauhan, A.K. Shah, M.R. Yadav, Recent advances in selective $\alpha_1$-adrenoreceptor antagonists as antihypertensive agents, Bioorg. Med. Chem. 16 (2008) 4759–4800.
[7] J.B. Bremner, B. Coban, R. Griffith, K.M. Groenewoud, B.F. Yates, Ligand design for $\alpha_1$ adrenoceptor subtype selective antagonists, Bioorg. Med. Chem. 8 (2000) 201–214.
[8] M.Y. Li, K.C. Tsai, L. Xia, Pharmacophore identification of $\alpha_{1A}$-adrenoceptor antagonists, Bioorg. Med. Chem. Lett. 15 (2005) 657–664.
[9] I.J.A. MacDougall, R. Griffith, Selective pharmacophore design for $\alpha_1$-adrenoceptor subtypes, J. Mol. Graph. Model. 25 (2006) 146–157.
[10] N.J. Richmond, C.A. Abrams, P.R. Wolohan, E. Abrahamian, P. Willett, R.D. Clark, GALAHAD: 1. Pharmacophore identification by hypermolecular alignment of ligands in 3D, J. Comput. Aided Mol. Des. 20 (2006) 567–587.
[11] T. Klabunde, A. Evers, GPCR antitarget modeling: pharmacophore models for biogenic amine binding GPCRs to avoid GPCR-mediated side effects, Chembiochem 6 (2005) 876–889.
[12] G.H. Kuo, C. Prouty, W.V. Murray, V. Pulito, L. Jolliffe, P. Cheung, S. Varga, M. Evangelisto, J. Wang, Design, synthesis, and structure–activity relationships of phthalimide-phenylpiperazines: a novel series of potent and selective $\alpha_{1a}$-adrenergic receptor antagonists, J. Med. Chem. 43 (2000) 2183–2195.
[13] G.H. Kuo, C. Prouty, W.V. Murray, V. Pulito, L. Jolliffe, P. Cheung, S. Varga, M. Evangelisto, C. Shaw, Design, synthesis and biological evaluation of pyridine-phenylpiperazines: a novel series of potent and selective $\alpha_{1a}$-adrenergic receptor antagonist, Bioorg. Med. Chem. 8 (2000) 2263–2275.
[14] K. Nanda, K.S. Naruganahalli, S. Gupta, S. Malhotra, A. Tiwari, L.G. Hegde, S. Jain, N. Sinha, J.B. Gupta, A. Chugh, N. Anand, A. Ray, RBx 6198: a novel $\alpha_1$-adrenoceptor antagonist for the treatment of benign prostatic hyperplasia, Eur. J. Pharmacol. 607 (2009) 213–219.
[15] V.L. Pulito, X. Li, S.S. Varga, L.S. Mulcahy, K.S. Clark, S.A. Halbert, A.B. Reitz, W.V. Murray, L.K. Jolliffe, An investigation of the uroselective properties of four novel $\alpha_{1a}$-adrenergic receptor subtype-selective antagonists, J. Pharmacol. Exp. Ther. 294 (2000) 224–229.
[16] H. Khatuya, R.H. Hutchings, G.H. Kuo, V.L. Pulito, L.K. Jolliffe, X. Li, W.V. Murray, Arylpiperazine substituted heterocycles as selective $\alpha_{1a}$ adrenergic antagonists, Bioorg. Med. Chem. Lett. 12 (2002) 2443–2446.
[17] C. Sorbi, S. Franchini, A. Tait, A. Prandi, R. Gallesi, P. Angeli, G. Marucci, L. Pirona, E. Poggesi, L. Brasili, 1,3-Dioxolane-based ligands as rigid analogues of naftopidil: structure-affinity/activity relationships at $\alpha_1$ and 5-HT$_{1A}$ receptors, Chem. Med. Chem. 4 (2009) 393–399.
[18] X. Li, K.A. McCoy, W.V. Murray, L. Jolliffe, V. Pulito, Novel heterocycles as selective $\alpha_1$-adrenergic receptor antagonists, Bioorg. Med. Chem. Lett. 10 (2000) 2375–2377.
[19] B. Lagu, Identification of $\alpha_{1A}$-adrenoceptor selective antagonists for the treatment of benign prostatic hyperplasia, Drugs Future 26 (2001) 757.
[20] H. Khatuya, V.L. Pulito, L.K. Jolliffe, X. Li, W.V. Murray, Novel thiophene derivatives for the treatment of benign prostatic hyperplasia, Bioorg. Med. Chem. Lett. 12 (2002) 2145–2148.
[21] M.C. Menziani, M. Montorsi, P.G. De Benedetti, M. Karelson, Relevance of theoretical molecular descriptors in quantitative structure-activity relationship analysis of alpha1-adrenergic receptor antagonists, Bioorg. Med. Chem. 7 (1999) 2437–2451.
[22] E. Patane, V. Pittala, F. Guerrera, L. Salerno, G. Romeo, M.A. Siracusa, F. Russo, F. Manetti, M. Botta, I. Mereghetti, A. Cagnotto, T. Mennini, Synthesis of 3-arylpiperazinylalkylpyrrolo[3,2-d]pyrimidine-2,4-dione derivatives as novel, potent, and selective $\alpha_1$-adrenoceptor ligands, J. Med. Chem. 48 (2005) 2420–2431.
[23] A. Leonardi, D. Barlocco, F. Montesano, G. Cignarella, G. Motta, R. Testa, E. Poggesi, M. Seeber, P.G. De Benedetti, F. Fanelli, Synthesis, screening, and molecular modeling of new potent and selective antagonists at the $\alpha_{1d}$ adrenergic receptor, J. Med. Chem. 47 (2004) 1900–1918.
[24] O. Dror, D. Schneidman-Duhovny, Y. Inbar, R. Nussinov, H.J. Wolfson, Novel approach for efficient pharmacophore-based virtual screening: method and applications, J. Chem. Inf. Model. 49 (2009) 2333–2343.
[25] X. Li, W.V. Murray, L. Jolliffe, V. Pulito, Novel arylpiperazines as selective $\alpha_1$-adrenergic receptor antagonists, Bioorg. Med. Chem. Lett. 10 (2000) 1093–1096.
[26] S. Wold, Validation of QSAR's, Quant. Struct. Act. Relat. 10 (1991) 191–193.
[27] R.D. Cramer, D.E. Patterson, J.D. Bunce, Comparative molecular field analysis (CoMFA). 1. Effect of shape on binding of steroids to carrier proteins, J. Am. Chem. Soc. 110 (1988) 5959–5967.
[28] S.J. Cottrell, V.J. Gillet, R. Taylor, D.J. Wilton, Generation of multiple pharmacophore hypotheses using multiobjective optimisation techniques, J. Comput. Aided Mol. Des. 18 (2004) 665–682.
[29] GALAHAD® Manual, SYBYL, version 8.1, Tripos Inc., Louis, USA, 2008.
[30] L. Betti, M. Floridi, G. Giannaccini, F. Manetti, C. Paparelli, G. Strappaghetti, M. Botta, Design, synthesis, and $\alpha_1$-adrenoceptor binding properties of new arylpiperazine derivatives bearing a flavone nucleus as the terminal heterocyclic molecular portion, Bioorg. Med. Chem. 12 (2004) 1527–1535.
[31] N. Hamaguchi, T.A. True, D.L. Saussy, P.W. Jeffs, Phenylalanine in the second membrane-spanning domain of $\alpha_{1A}$-adrenergic receptor determines

subtype selectivity of dihydropyridine antagonists, Biochemistry 35 (1996) 14312–14317.

[32] M. Cocchi, M.C. Menziani, F. Fanelli, P.G. de Benedetti, Theoretical quantitative structure-activity relationship analysis of congeneric and non-congeneric $\alpha_1$-adrenoceptor, J Mol Struct: Theochem. 331 (1995) 79–93.

[33] P. Venturelli, M.C. Menziani, M. Cocchi, F. Fanelli, P.G. de Benedetti, Molecular modelling and quantitative structure-activity relationship analy-sis using theoretical descriptors of, J Mol Struct: Theochem. 276 (1992) 327–340.

[34] J. Kirchmair, P. Markt, S. Distinto, G. Wolber, T. Langer, Evaluation of the per-formance of 3D virtual screening protocols: RMSD comparisons, enrichment assessments, and decoy selection-What can we learn from earlier mistakes? J. Comput. Aided Mol. Des. 22 (2008) 213–228.